Acoustic diffraction patterns from regular to fractal structures: application to the Sierpinski carpet

Philippe Woloszyn

Acoustic diffraction patterns from fractal to urban structures: Applications to the Sierpinski triangle and to...

Chapter · January 2005

DOI: 10.1007/1-84628-048-6_7

CITATIONS
2

READS
12

1 author:

Philippe Woloszyn
French National Centre for Scientific Research
100 PUBLICATIONS **209** CITATIONS

SEE PROFILE

Acoustic diffraction patterns from regular to fractal structures: application to the Sierpinski carpet

Philippe Woloszyn

Acoustic dept., Cerma Lab., UMR CNRS 1563, E.A.N., BP 81931
F-44319 Nantes Cedex 3, France
E-mail: philippe.woloszyn@cerma.archi.fr

Abstract. The concept of fractal geometry, introduced by Mandelbrot has been explored in diverse areas of science, including acoustics [1]. First part of this work relates the properties of far-field Fraunhofer region diffraction in wave acoustics for characterizing reflection on a periodic regular indented plane. Diffusion prediction of a self-similar structure, the Sierpinski carpet, is then developed through the computation of its spatial Fourier transform. Scattering intensity computation results show that after propagation of a coherent plane wave through the structure, the resulting acoustical field displays fractal properties itself, showing a self-similar structure of the reflected signal. This computational approach of the Sierpinski carpet's scattering properties will lead us to develop, in a near future, an acoustic angular scattering measurement process, applied to a Sierpinski tetrahedron 3-D scale model.

1 Introduction

The aim of this work is to define an acoustic diffraction pattern computation model from varying geometry complexities, of regular or fractal structures [2]. To do this, we'll develop twice analytical and numerical approaches of the far-field diffraction models, based on electromagnetism diffraction analogy [3]. Founding this approach, Bragg's law and Fraunhofer's model describe the field conditions for constructive and desctructive interferences, which is produced from strong diffraction. Considering diffusive structures as families of parallel planes running in different directions, each plane acts like a slightly reflective mirror, reflecting a tiny fraction of the incident acoustic wave. When in phase, those reflections lead to diffraction interferences production [4].

2 Diffraction conditions

Diffraction of a wave by a periodic structure is due to phase differences that result in constructive and destructive interference. This phenomenon can occur when waves pass through a periodic structure if the repeat distance is similar to the wavelength of the waves. Observation of diffraction patterns when acoustic waves pass through complex structures is here completed through the nature of those waves, involved diffraction process.

Diffraction patterns are most obvious when the incoming waves are coherent, which means that the phase of the sinusoidal pattern of the acoustic fields is deterministic. Coherence has two domains: spatial and temporal. Consequently, knowledge of the field phase at some point in space and/or time determines the phase at other points in space and/or time. For spatially coherent sound, the phase difference $\Delta\varphi \equiv \varphi 1 - \varphi 2$ of the field measured at two different points in space at the same time separated by a vector distance Δr remains constant for all times. If the phase difference measured at the same location at two different times separated by $\Delta t \equiv t1 - t2$ is the same for all points in space, therefore, the sound is temporally coherent.

2.1 Wave coherence

The Fresnel (near-field) diffraction region occurs when the distance between the structure and the reception plane is small compared to the size of the structure. Fresnel diffraction pattern involve an hemispheric wavefront to reach the reflective structure, which means uncoherent incoming waves defining a non-deterministic acoustic field into twice spatial and temporal domains [5].

Otherwise, if viewed at a large distance compared to the extent of the object, the sound may be accurately modeled as plane waves with different wavefront tilts. This occurs in the Fraunhofer diffraction region as seen Figure 1:

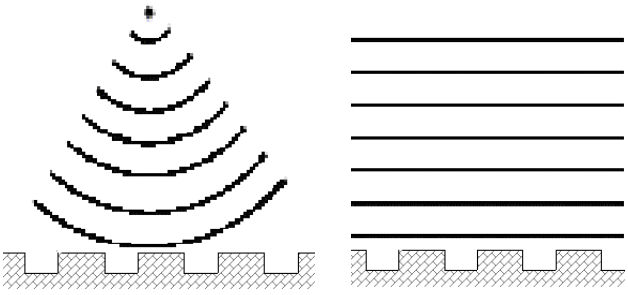

Fig. 1. Fresnel (near-field) and Fraunhofer (far-field) diffraction regions

The diffraction length, known as the Rayleigh distance *Dr*, marks the transition between the near-field and the far-field regions of the waves.

$$D_r = \frac{2D^2}{\lambda} \cdot \quad (1)$$

Considering the mean path *D* of the reflecting structure, most of the reflected energy of wavelength λ is diffracted through an angle of the order $\alpha = \lambda/D$ radians from its original propagation direction. When the wave have travelled a distance *r* from the plane, about half of the reflected energy will have left the plane structure by the geometric shadow if $D/R = \alpha$. Consequently, the majority of the propagating energy in the "far field region" at a distance greater than the Rayleigh distance will be diffracted energy with polar radiation pattern. Physically, the equations for Fraunhofer and Bragg diffraction are similar and embody the same functional dependence on the distance *r* of the structure, incident wavelength λ, and scattering angle α.

2.2 Interferences production

Within wave acoustics, interferences are described through the expression for the sum of two sinusoidal temporal oscillations of the same amplitude *A* and different frequencies $f1 = 2\pi/\omega 1 = c/\lambda 1$ and $f2 = 2\pi/\omega 2 = c/\lambda 2$, with λ, wavelength of the incoming wave :

$$\mathrm{A}\cos[\omega 1\mathrm{t}] + \cos[\omega 2\mathrm{t}] = 2\mathrm{A}\cos\left[\frac{(\omega 1 + \omega 2)}{2}t\right].\cos\left[\frac{(\omega 1 - \omega 2)}{2}t\right] \cdot \quad (2)$$

In order to generalize waves travelling in any direction, we introduce the 3-D wavevector:

$$k = [\mathrm{kx}, \mathrm{ky}, \mathrm{kz}] = \sqrt{\mathrm{k_x^2} + \mathrm{k_y^2} + \mathrm{k_z^2}} = \frac{2\pi}{\lambda} \ , \quad (3)$$

pointing in the direction of travel of the wave. Thus, the length of the wavevector is proportional to $1/\lambda$. Thus, the equation for a travelling wave in 3-D space becomes:

$$\mathrm{f}[\mathrm{x}, \mathrm{y}, \mathrm{z}, \mathrm{t}] = \mathrm{f}[\mathrm{r}, \mathrm{t}] = \mathrm{A}\cos[\mathrm{k_x x} + \mathrm{k_y\ y} + \mathrm{k_z\ z} - \omega.\mathrm{t}] = \mathrm{A}\cos[\mathrm{k.r} - \omega.\mathrm{t}] \ . \quad (4)$$

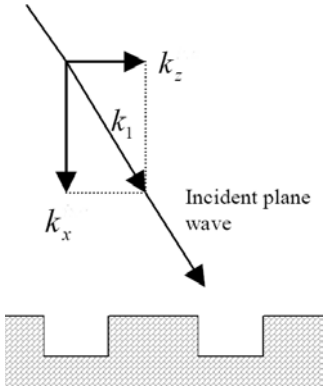

Fig. 2. (x, z) incoming wave vector on a regularly indented plane

A 3-D wavefront can exhibit a periodic variation in the phase $\varphi\ [r, t] = kr - \omega t$, even when the wave is monotone as: $\omega 1 = \omega 2 = \omega \rightarrow \lambda 1 = \lambda 2 = \lambda$. If sound from a single source is reflecting into two indents at different heights, Rayleigh's principle indicates that the sound through the two indents will "spread" and recombine. When viewed at a single location, the two sound "rays" with the same wavelength will recombine with different wavevectors such that $|k1| = |k2| = |k|$.

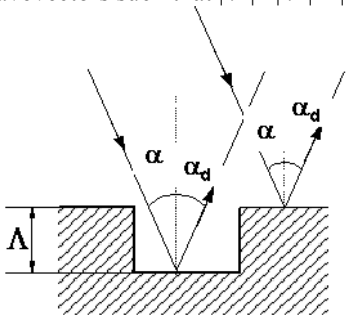

Fig. 3. Interference geometry into an indent

2.3 Rayleigh's principle and Bragg's Law

Rayleigh's principle proposes a phase calculation between two acoustic rays, which takes the source incidence angle into account [4]. The path difference Δd between two rays with wavelength λ and incidence angle α regarding a surface with depth Λ provides the following phase grating calculation between the two rays:

$$\Delta\alpha = \Delta d\ (2\pi / \lambda) = \cos\alpha\ (4\ \pi\ \Lambda / \lambda)\ , \qquad (5)$$

with the path difference $\Delta d = 2\Lambda\cos\alpha$.. For a weak path difference Δd, rays are coherent and the acoustic wave is specularly reflected. Increasing Δd interferes with rays, till $\Delta d = \pi$, so that no energy is displayed in the specular direction : sound energy is then diffused. Rayleigh criterion defines the limit between specular and

diffuse behavior of an incident source, corresponding to the structure depth indentations as : $\Lambda < l/8\cos\alpha$..

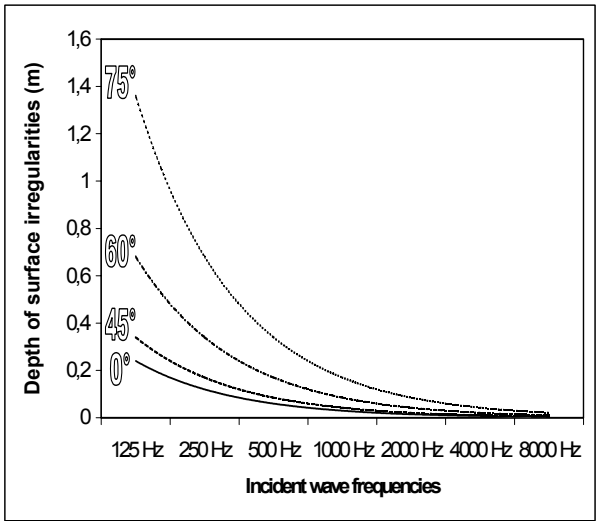

Fig. 4. Rayleigh criterion: limits between specularity and diffusion, as a function of frequency, incidence angle, and structure intation depths.

The specular reflection zone is defined in the lower part of the curves, taking the frequency and the angle of the incident wave into account. In interferences conditions, the propagation directions specified by the unit vectors $\mathbf{v}(d) = (\phi_d, 0, \gamma_d)$ for a given regular plane division, repeating ν times a spatial unit of depth Λ are defined as the characteristic directions of scattering:

$$\sin\alpha_d = \frac{p\lambda}{2\nu\Lambda} - \sin\alpha \quad , \tag{6}$$

where α_d is the grazing diffraction angle made by vectors $\mathbf{v}(d) = (\phi_d, 0, \gamma_d)$ in the direction $0x$, with $\phi_d = \cos\alpha_d$ and $\gamma_d = \sin\alpha_d$, , and p the diffraction order. For $\Lambda = 0$, equality between incident and reflected angle remain true, providing specular conditions specification. We can note here that, ignoring the specular component $\sin\alpha$, the first term of the previous equation can be compared to Bragg's Law, leading to the following expression:

$$\sin\alpha = \frac{p\lambda}{2\Lambda}, \tag{7}$$

where the integer p is the diffraction order, Λ, the distance between two reflection planes, λ, the wavelength of the incident beam and α its incidence angle.

Moreover, the two-dimensional polar response of a given indented surface can be expressed through the diffraction orders (*p, q*), taking the angles of incidence and diffraction into account:

$$\sqrt{p^2+q^2} = \nu\Lambda \frac{\sin\alpha_d + \sin\alpha}{\lambda} \ . \qquad (8)$$

2.4 Interference geometry.

The interference conditions can be expressed by defining the phases of the incident wave vector k_0 and the diffracted vector k, which both have an amplitude equal to the reciprocical of the wavelength. In order to calculate the phase of the diffracted wave, taking the path lengths difference $\Delta d = 2\nu\Lambda \cos\alpha$ into account, we will consider the difference between the path of the sound wave along the incident beam $k_0 r$ and its path along the diffracted beam kr (figure 5). By expressing this path length difference $\Delta d = k_0 r - kr$, the overall diffraction phase as:

$$\Delta\varphi = 2\pi(k - k_0)r \qquad (9)$$

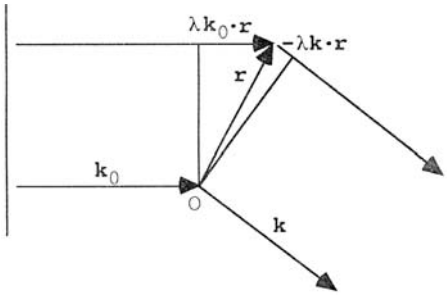

Fig. 5. Phase geometry

Considering $|r|\cos\alpha$ the component of r in the direction of the diffraction vector s, all points with the same value of sr are lying on a plane perpendicular to vector s, allowing the same diffraction phase (figure 6).

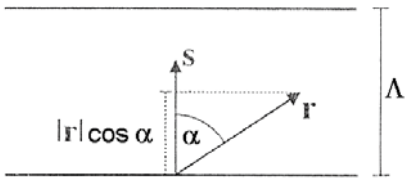

Fig. 6. Diffraction geometry

Consequently, as the length of the diffraction vector $|s|$ is equal to the spatial amplitude Λ (indentation depth), sr is a periodic function in the spatial domain,

involving dimensions of the diffraction planes (indentation surfaces), and diffraction from any point at distance r of the structure will have a phase of $sr = 2\pi\nu r$ in the space domain.
In order to define reflection systems geometries in terms of their scattering functions, we'll define the incident sound wave in the z-direction as equation (10).
For a singly periodic structure which bellows uniform indentations of amplitude Λ, the two dimensional acoustic field satisfies the following Fourier series [6]:

$$F(k) = \sum_{\infty} G_0(k) e^{-(\Lambda + j2\pi\nu r)} \tag{10}$$

Each of the terms of the series in previous equation is a spatial harmonic with period ν. The density-density correlation function G_0 is a main parameter of the scattering intensity of the structure. For an incident plane wave, equation (10) provides result of scattering from a periodic structure as an infinite sum of plane scattered waves, mostly harmonics.

After reflection on the plane structure, amplitude and phase are found to be independent of the precise waveform of the incident wave. Moreover, the diffractance function at distance r of the structure $g(r)$ is a characteristic property of the structure, defining the interfering behaviour of the scattered wave.
However, $g(r)$, the angular distribution function along a characteristic direction of scattering informs on the wave disturbance at a distance r from the object as:

$$g(\mathbf{r}) = \frac{1}{m^2}(G_0(\mathbf{r}) - \overline{m}\ \rho(\mathbf{r})) \tag{11}$$

2.5 Fraunhofer diffraction pattern

The mathematical relationship between the shape and size of the wave output relative to that of the spatial structure input is a Fourier transform [7]. As the Fraunhofer diffraction pattern of the structure is related to the Fourier Transform of the diffractance function $g(r)$, at large distances from the sound source, the far field or Fraunhofer diffraction region involves the diffracted sound pattern as variable in proportion to the reciprocal of the structure dimensions. Then, for the same energy input pattern f, the one-dimensional diffraction pattern in the Fraunhofer region has the angular distribution form:

$$g(r) \propto \int_{\infty} f(\alpha) \exp\left[-\frac{2i\pi\alpha r}{\lambda z}\right] d\alpha \tag{12}$$

The effect of incident plane wave scattering is the creation of far-field secondary waves. These waves, arising from each point on the structure, travel in all directions giving rise to complex distributions of amplitude and phase.

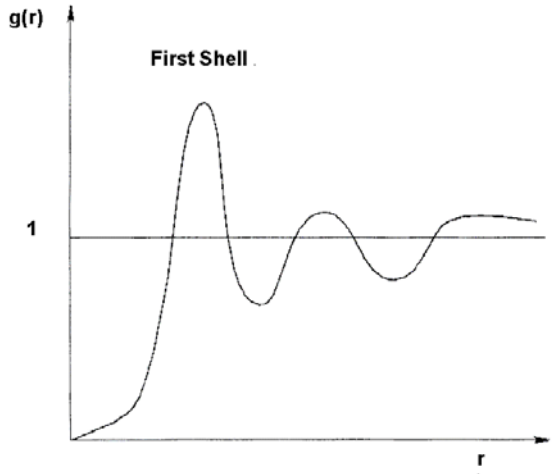

Fig. 7. Typical angular distribution function. The first shell represents the main density function at a distance *r* of the structure.

Diffractance formulation (12) implies the density-density correlation function $G_0 = \langle m(o)m(\mathbf{r})\rangle$, which is the second moment of energy density taken between *0* and *r*. Square of the average density:

$$\overline{m} = \sum_i \rho(\mathbf{r}_i) \tag{13}$$

constitutes the limit of the density-density correlation function G_0 when $\mathbf{r} \to \infty$: $G_0(\mathbf{r}) \to \overline{m}^2$ and $g(\mathbf{r}) \to 1$, where a perfectly flat angular distribution function signs the specular field behaviour. This diffractance function *g(r)* defines the scattering intensity of the structure for a defined angle as:

$$I_q(r) = \int_i G_0(\mathbf{r})^{-iqr} dr \tag{14}$$

This function describes secondary acoustic waves leaving the scattering structure at a specified angle and arriving at a particular point, creating scattering sidelobes. The complex amplitude at this point is obtained by adding the individual contributions from primary and secondary sources of amplitude *g(r)*, involving the different path lengths of the travel to the reception point. Thus, the contribution from the element *dr* at a distance *r* is specified through the following one-dimensional intensity distribution, which is a major parameter of the Fraunhofer diffraction pattern:

$$I(r) = \left| \int_\infty g(r).\exp(-i\frac{qr}{f})dr \right|^2 . \tag{15}$$

The expression may be compared with the one-dimensional Fourier Transform of the diffractance function $g(r)$ as:

$$\overline{g}(k_r) = \int_{\infty} g(r).\exp(-i\,vr)dr \tag{16}$$

where $v=q/f$ is the spatial period of the indented structure. Taking equations (15) and (16) into account, the measured intensity $I(r)$ and the square of the modulus of the structure diffractance Fourier transform are identical:

$$I = |\overline{g}|^2 = |F_n|^2 \prod_i \left(\frac{\sin 2\pi k r_i}{2\pi k r_i} \right)^2 \tag{17}$$

This identity allows the expression of the scattering intensity I as a function of the structure factor of the indented plane, implying the characteristic interference function $sinx/x$, for a frequency $f = 1/2\pi k$ as shown figure 8:

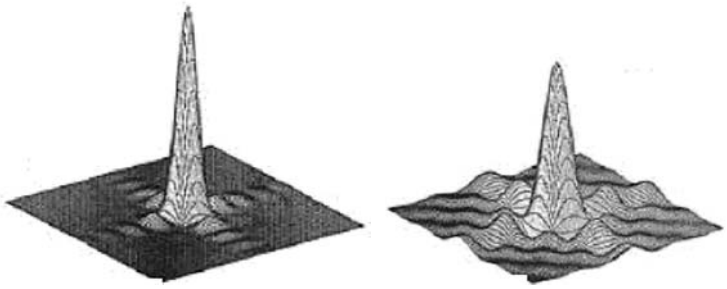

Fig. 8. Typical Fraunhofer diffraction patterns

The structure factor Fn is the Fourier transform of the scatterers of equal strength on all points at distance r of the diffraction plane. Continous expression of this previous equation involves structure angular distribution as:

$$F_n(r) = \int_{space} \overline{g}(k_r) \exp(2\pi i k_r)dr \tag{18}$$

As shown equation (18), the diffraction pattern is defined as the Fourier transform of the structure angular density.

3 Application to the Sierpinski carpet structure

In this section, we will apply the Fraunhofer diffusion formalism to a well-known two-dimensional structure, the Sierpinski carpet, in order to explore it behaviour from a wave acoustical solicitation. To do so, we will express its Fourier transform trough introduction of an iterative term into the structure factor.

3.1 Iterative structure factor

As the structure factor of the Fourier Transform of a multiplicative signal of level *n* can be written as either a product of n periodic functions $H_i\,(r)(\,i = 1, 2, \ldots, n)$ with frequencies D_{i-1}, or a product of *n* scaled replicas of the structure factor of the first level $H_1(u)$ [8]:

$$F_n(r) = \prod_{i=1}^{n} H_i(r) = \prod_{i=1}^{n} H_1(rD_{i-1}) \tag{19}$$

Thus, the level n one-dimensional structure factor, constructed through an iterative procedure, can be defined as:

$$H_n(r) = \sum_{i=0}^{n} f_1 H_{n-1}(r) * \delta(r - \nu D_{i-1}) = \sum_{i=0}^{n} f_1 H_{n-1}(r - \nu D_{i-1}) \tag{20}$$

When the initiator is a square and the generator *f1* its bottom-right quadratic subtraction complement, the Sierpinski carpet set is then obtained through the following iterative procedure:

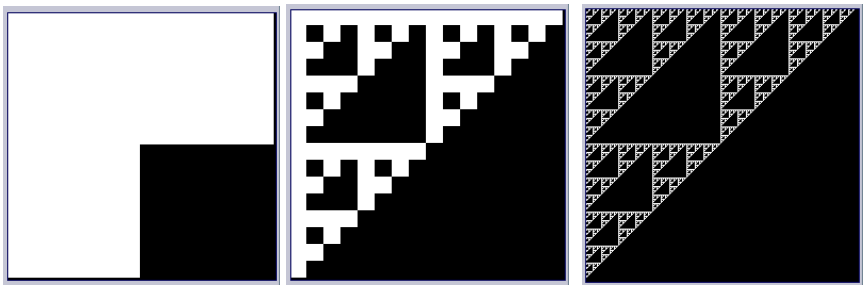

Fig. 9. Sierpinski triangle Generator, and 8 th & 16 th iteration levels.

Alternatively, if *Hn(r)* in the form (20) is introduced in the Fourier integral, then the structure factor can be represented by the following Fourier series:

$$F_n(r) = \sum_{i=0}^{n} \exp(-2\pi i r / \nu_i) = \exp\left[-\pi i D_{i-1}\right] \frac{\sin(2\pi k r)}{\sin(\pi \nu_i r)}\ , \tag{21}$$

where ν_i is the spatial period of the structure at iteration level $i=n$, with scaling coefficients $Di-1$ *for* $i = 1, \ldots, n$..

The structure factor *Fn(r)* is a complex function, as the initiator as well the generator matrix can take complex values. It is know that such as multiplicative cascades for real non-negative values of the generator matrix produce regular fractals [9].

We can observe a similarity in the construction of the multiplicative reflection structure itself and its Fourier Transform. Indeed, the structure factors in both cases are constructed as a product of n scaled replicas of the periodic signals with scaling coefficients $Di-1$.

3.2 Results and discussion

As an indicator of the indentation frequency, the Fourier transform discriminates clearly the structure of the reflection surface, revealing the spatial occurrences of the roughness peaks.

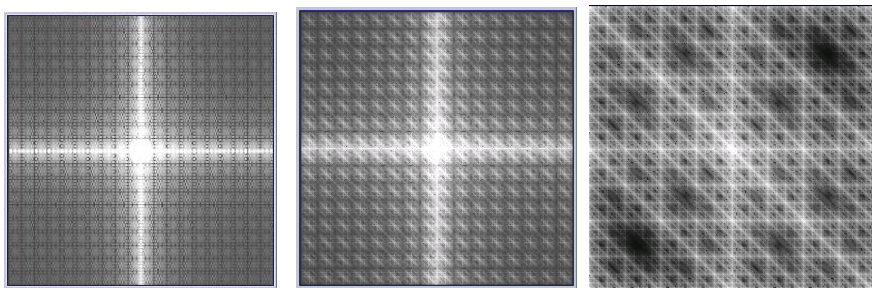

Fig. 10. Space Fourier Transform of the Sierpinski carpet Generator, 8 th & 16 th iteration

Fourier transform of the structure shows quasiperiodic behaviour of the structure factor, at every iteration if the shape. In addition, we can note that when iteration levels goes to infinite, the fractal structure becomes invariant for its Fourier transform. The angular scattering distribution function is defined through the structure factor computation of the surface, and indicates the fractal scattering behaviour for a particular direction of the incident wave:

$$I = \left| \exp\left[-\pi i D_{i-1} \right] \frac{\sin(2\pi r)}{\sin(\pi v_i r)} \right| \prod_i \left(\frac{\sin 2\pi k r}{2\pi k r} \right) \tag{22}$$

The scattering intensity distribution leads to define the Fraunhofer diffraction patterns of each structure iteration level figure 11:

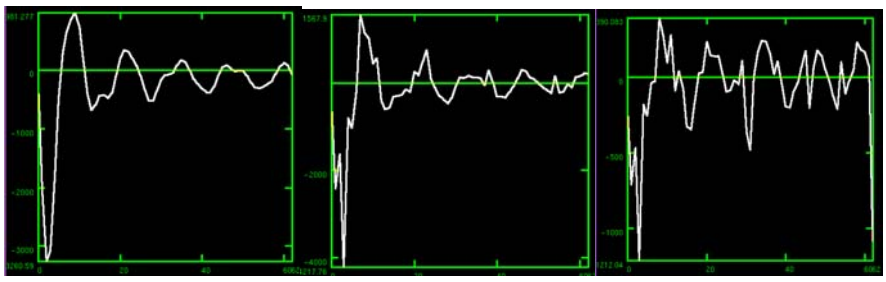

Fig. 11. Sierpinski carpets scattering angular distribution functions at $\pi/2rd$ for $v=\lambda$ (*structure distance* vs. *power density function*)

We can easily discriminate an anomalous quasiperiodic behaviour of the scattering angular and spatial factors, even when the characteristic Fraunhofer diffraction region pattern remains obvious.

The angular density function remains quasi-periodic at any distance of the carpet, signing a quasi-perfect diffusive structure. The angular distribution of propagating energy will then no longer depend on the distance from the plane structure.
Moreover, the spatial scattering distribution function offers a tridimensional representation of the scattering distribution function, showing the angular and distance distribution's 3-D map of the surface's scatterers density:

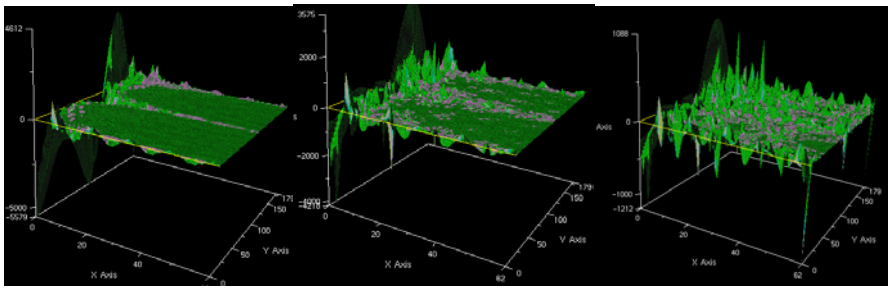

Fig. 12. Sierpinski carpets spatial scattering distribution functions (*structure distance* vs. *diffraction angle* vs. *power density function*)

Results shows a high spatial diffractance persistence for high-level iterated Sierpinski carpet. This behaviour traduces an important diffusion capacity of the Sierpinski structure at high iteration levels.

Spatial scattering distribution function data also provide scattering intensity cross-distribution plot, as presented for the three iteration levels of the carpet:

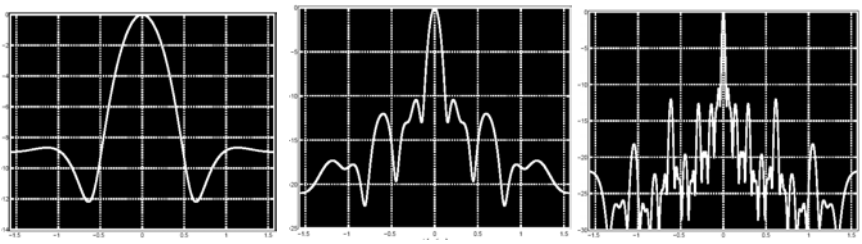

Fig. 13. Sierpinski carpets scattering intensity cross-distributions (*diffraction angle* vs. *power density function*)

As expected, the Sierpinki carpet far field scattering intensity cross-distribution shows self-similar diffraction patterns for several spatial frequency bands: after propagation of a coherent plane wave through this fractal grating, the computed acoustic field has fractal properties.

This diffraction pattern may be interpreted as the spatial filter response of the analysed structure. The location of mainlobe peak tells in which direction we get maximum response of the spatial structure from an acoustical solicitation. The mainlobe (highest peak) is then similar to the pass-band in a spatial filter, which diffracts acoustic energy in these directions.

4 Conclusion

It has been shown that diffusion capacity of a complex plane can be directly computed from the Fourier transform of its spatial structure. Applied to a fractal plane structure, the resulting spatial intensity distribution reveals the self similar behaviour of the scattered acoustic field angular distribution. Moreover, this Fraunhofer diffraction region characterisation allows scattering prediction for many types of spatial configurations, under condition of interference acoustic field, that means spatial / temporal frequencies ratio.

This powerful computation tool can also be applied to all types of complex geometries, including architectural (concert hall diffusers) and urban (façade indentations) configurations, in order to predict their far-field diffusion behaviour [10].

References

1. Mandelbrot B B 1982 The Fractal Geometry of Nature (San Francisco, CA: Freeman)
2. Woloszyn P. Is Fractal Estimation of a Geometry worth for Acoustics ?, Emergent Nature, M. M. Novak (ed.), World Scientific Publishing Singapore, 2002, pp.423-425.
3. Beckmann P., Spizzichino A., 1987 The Scattering of Electromagnetic Waves from Rough Surfaces, Artec House, *INC*, Norwood.
4. Lord Rayleigh, The theory of Sound, Vol. 2, Dover ed, New-york, 1945, pp. 89-96.
5. Hamilton M. F., Sound beams, Chap. 8 in Nonlinear Acoustics, M. F. Hamilton and D. T. Blackstock,, eds. Academic Press, Boston, 1998, pp. 233–261
6. Woloszyn P., Fractal Scattering Indicators for Urban Sound Diffusion, Thinking in Patterns: Fractals and Related phenomena in Nature , M. M. Novak (ed.), World Scientific Publishing, Singapore, pp. 221-232.
7. Hollander and al., Dynamic Structure Factor in a Random Diffusion Model, Journal of Statistical Physics, Vol.76, **5:6**, 1994.
8. Alieva T., Calvo M-L.: Paraxial diffraction on structures generated by multiplicative iterative procedures, J. Opt. A: Pure Appl. Opt. 5, IOP Publishing Ltd, (2003) 324–328
9. Umberto Marini Bettolo Marconi and Alberto Petri Domain growth on self-similar structures, phys. Rev. Vol. 55, N°2 (1997)
10. Woloszyn P., Suner B., Bachelier J.: Angular characterization of the urban frontages diffusivity factor, 17th International Congress of Acoustics, Rome, Italy, 2001.